

Exposure of Silver to Atomic Oxygen

A. de Rooij

Head of Materials Technology Section
Product Assurance and Safety Department
European Space Agency-ESTEC
Noordwijk, The Netherlands

Keywords:

atomic oxygen, corrosion, space, low earth orbit, LEO, ATOX, flight testing, on-ground testing

Abstract

The corrosion in space is described by the effect of atomic oxygen on several materials. The metal which was most affected is silver. Silver oxidizes according to a linear-parabolic law and due to the thermal stresses the oxide layer continuously breaks up, resulting in a linear degradation.

Atomic oxygen not only attacks materials in the line of sight of the ram flux, but also by reflected atomic oxygen.

The transport of oxygen through the oxide layer is modelled using two transport mechanisms, namely gas flow through micro-pores and Fickian diffusion. The interfacial reaction between oxygen and silver is taken as linear, resulting in a linear-parabolic oxidation with flux and time. The model results in a low-temperature oxidation by gas flow while at higher temperature the diffusion mechanism controls the kinetics of the oxidation.

Introduction

Materials for use in space applications in low earth orbit and exposed to the hostile combination of atomic oxygen and thermal cycling have to be screened for their susceptibility to withstand this environment over very long periods. Atomic oxygen is produced by the photo-dissociation of molecular oxygen in the upper atmosphere by solar radiation of wavelength less than or equal to 243 nm[1]. It is the main constituent of the residual atmosphere in Low Earth Orbit (LEO) as illustrated in figure 1.[2] The oxygen atoms have a density of 10^7 to 10^8 atoms/cm³ at International Space Station (ISS) altitude (around 400 km) with a thermal energy of approx. 0.1 eV. The orbital atomic oxygen density can be calculated with the aid of the MSIS-86/CIRA Neutral Thermosphere Model of Hedin[3]

Referring to figure 1 one can see the dominant atmospheric constituent concentrations as a function of altitude. Space vehicles are orbiting with a velocity of 7.78 to 8 km/s at those altitudes. For satellite-gas collision interactions, this orbital velocity corresponds to impact gas energies of 0.34, 4.40 and 5.03 eV for hydrogen, nitrogen and oxygen atoms, respectively.

Concentrating only on the O-atoms and taking into account the solar activity the maximum and minimum atomic oxygen density as function of altitude is shown in figure 2. The atomic oxygen flux depends on the altitude, the solar activity, the orbital inclination and the time of year. The collision with the external surfaces of space vehicles, orbiting at a velocity of 8 km/s, results in a ram flux of 10^{14} - 10^{15} O-atoms/(cm²/s).

Experiments on metals were carried out during many STS flights, on LDEF, Eureka and on ground. The majority of the experiments were conducted on silver, while at the

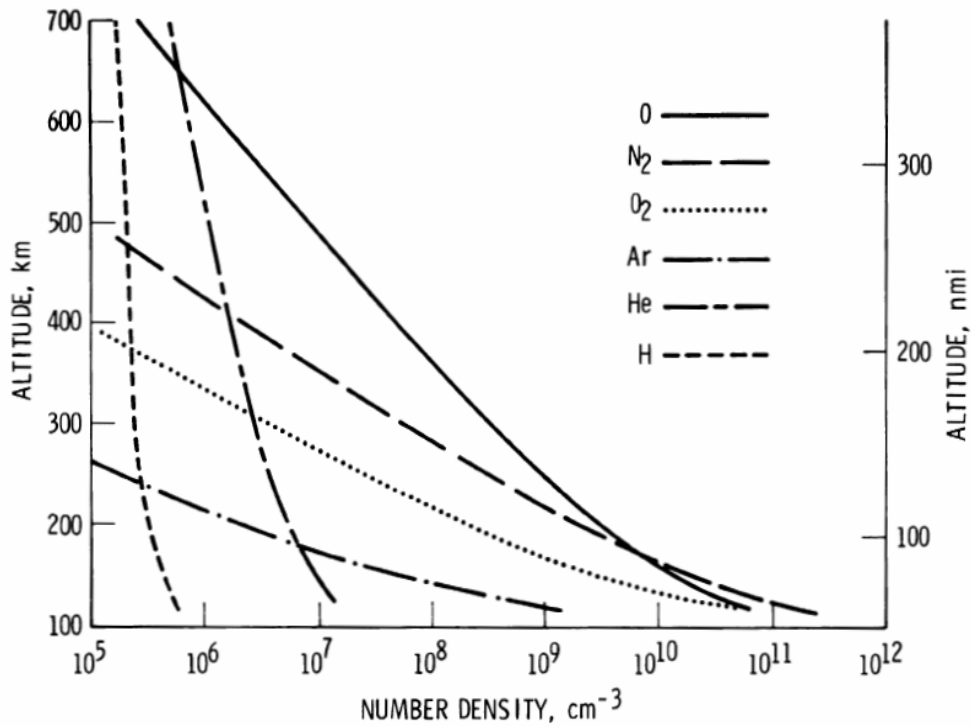


Figure 1: Atmospheric composition in Low Earth Orbit

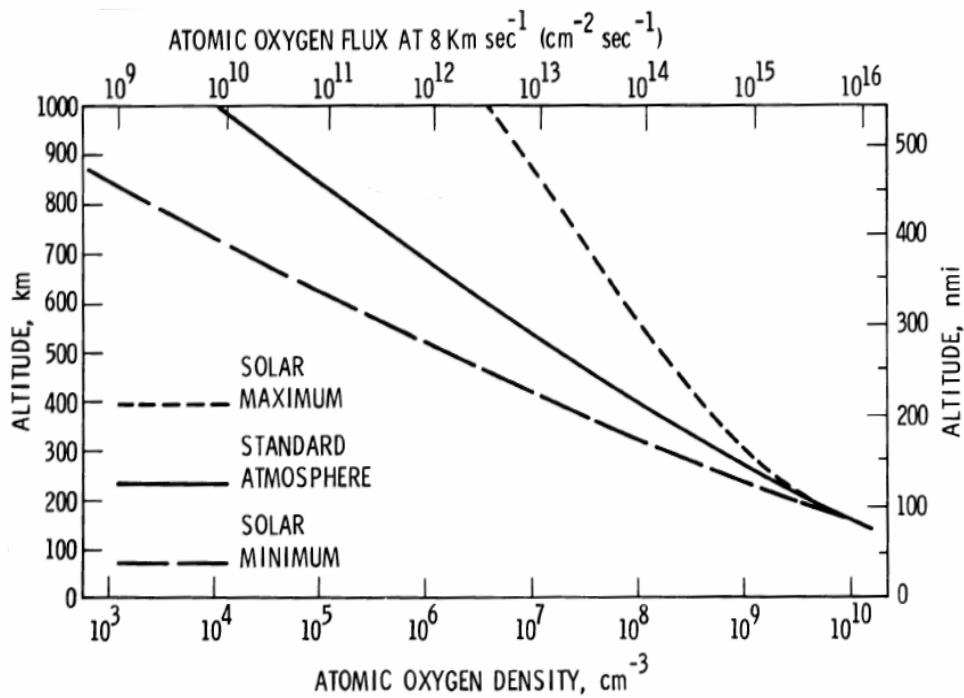


Figure 2: Atmospheric Atomic Oxygen density in Low Earth Orbit

time of the Hubble Space Telescope development silver was used as solarcell interconnectors. On-ground experiments were conducted in line with these ones and extended with other metals.

The oxidation of silver in atomic oxygen is essentially linear-parabolic as postulated by De Rooij[4] and experimentally confirmed by Chambers et.al[5]. The silver oxidizes until internal stresses in the oxide layer either to mechanical or thermal excursions causes the oxide layer to crack and eventually spall and flake off, leaving bare silver exposed to atomic oxygen again. This process repeats itself until the silver is completely oxidised.

Oxidation model

An oxide layer model was developed in [4] to predict the silver oxidation by atomic oxygen. This model will be extended and the approximations will be removed. The mechanism of oxide growth at increased temperatures is diffusion through the oxide layer along short circuit paths such as grain boundaries and lattice diffusion. As the diffusion is a temperature-controlled process, the observation of a substantial amount of oxidation at room temperature indicates a different oxidation process or at least a parallel process capable of oxidizing the metal in a parabolic manner and operational at low temperatures. The process responsible for the low temperature oxidation is known as gas flow through micro-pores.

Several mechanisms of gas transport through micro-pores can occur. These are free molecular flow (Knudsen flow), molecular flow, viscous flow and surface diffusion. At very low pressures where the mean free path of the oxygen atoms is larger than the dimensions of the pore, the wall collisions within the pore are more frequent than collisions between other oxygen atoms. This regime is called the free-molecular flow regime. The density of O-atoms in low earth orbit is approx. 10^8 atoms/cm³ and the mean free path is calculated ad 10^7 μm which is much larger then the expected pore dimension.

The number of atoms flowing through a pore is determined by the conductance of that pore. There are two aspects:

- 1) The rate at which atoms enter the pore
- 2) The probability that these atoms are transmitted though the system.

A gas with a density of n_1 at the entrance of a pore and a backflow at the other side gives a gasflow F_k of

$$F_k = \omega \bar{v} (n_1 - n_2) \quad (1)$$

where ω = a dimensionless probability factor
 \bar{v} = the mean velocity of the atoms in the pore

The atoms entering the pore loose their velocity due to scattering in the pores during the first wall collisions. Their speed is than reduced to \bar{v}

The expression for n_1 is then

$$n_1 = \frac{Nv}{\bar{v}} \quad (2)$$

where N = the atomic oxygen density
 v = velocity of the spacecraft
 Nv = ϕ = the flux of atomic oxygen on the spacecraft

$$\bar{v} = \sqrt{\frac{8RT}{\pi M}} \quad \text{from gas kinetic theory} \quad (3)$$

R = gas constant=8.314 J/(mol.K)

T = temperature

M = molecular mass

The probability factor ω depends on the geometry of the pore and is given by the Clausing factor

$$\omega = \left[1 + \frac{3}{16} \frac{L_r H}{A} \right]^{-1} \quad (4)$$

where L_r = the real length of the micropore

H = perimeter of the micropore

A = cross sectional area of the micropore

The pores have a certain path through the oxide layer and this can be related to the straight direct path y , which is the oxide thickness, by the tortuosity τ .

$$\tau = \frac{L_r}{y} \quad (5)$$

Only a percentage ε of the surface consists of open pores where the Knudsen flow can take place.

In summary we can write for the flow of oxygen atoms through porous layer by substituting eq. 2, 3 and 5 in eq. 1:

$$F_k = \varepsilon \left[1 + \frac{3}{16} \frac{Hy\tau}{A} \right]^{-1} \{ \phi - n_2 \bar{v} \} \quad (6)$$

Diffusion through short circuits and lattice is governed by the concentration difference of the diffusion atoms at both sides of the porous layer. At the front side the density is given by eq. 2. At the metal side the density is n_2 .

The differential flux of atoms through the oxide layer (with the exception of the pores) is then written as:

$$F_d = \frac{D(1-\varepsilon)}{y} \left\{ \frac{\phi}{\bar{v}} - n_2 \right\} \quad (7)$$

$$\text{where } D = \text{diffusion coefficient} = D_0 \exp\left(\frac{-Q}{RT}\right)$$

The oxygen atoms reaching the metal surface will finally react with the base metal and form the oxide. This type of reactions is usually linear and with an oxide flux of:

$$F_o = Kn_2 \quad (8)$$

$$\text{where } K = \text{rate of metal oxidation} = K_0 \exp\left(\frac{-Q}{RT}\right)$$

For a steady state situation the oxygen flux through the pores F_k and from the diffusional transport F_d must be equal to the oxide flux F_o produced by the oxidation:

$$F_k + F_d = F_o \quad (9)$$

The unit for the oxide flux F_o is related to the oxide growth rate by

$$\left(\frac{dy}{dt}\right)_{ox} = C\Omega_r F_o \quad (10)$$

Where

C = conversion factor from atoms/cm³ to cm³ metal-oxide
= 1.70520 10⁻²³ for silver

Ω_r = real volume ration oxide/metal due to porosity

$$\Omega_r = \frac{\Omega_{th}}{(1-\varepsilon)} \quad (11)$$

In which Ω_{th} = theoretical volume oxide/metal ratio = 1.6 for silver

Substituting eq. 6, 7 and 8 into eq. 9 enables us to express the generally unknown n_2 , in the gasflow and diffusion expressions and using this in eq. 10 one obtains the master equation for the oxide growth governed by the gasflow and diffusion transport mechanism through the oxide layers.

$$\left(\frac{dy}{dt}\right)_{ox} = \frac{CK \frac{\Omega_{th}}{(1-\varepsilon)} \frac{\phi}{\bar{v}}}{1 + \frac{\frac{\varepsilon \bar{v} y}{3Hy\tau} + D(1-\varepsilon)}{1 + \frac{3Hy\tau}{16A}}} \quad (12)$$

Equation 12 can solved using standard methods and after some algebra this results in:

$$\frac{\Omega_{th}CK\phi.t}{\bar{v}(1-\varepsilon)} = y^2 \frac{KP_c}{2W} + y \left\{ 1 + \frac{K}{W} - \frac{KP_c D_\varepsilon}{W^2} \right\} - V \left\{ \frac{K}{W} - \frac{KP_c D_\varepsilon}{W^2} \right\} \quad (13)$$

Where $P_c = \frac{3H\tau}{16A}$

$D_\varepsilon = D(1-\varepsilon)$

$W = \varepsilon \bar{v} + P_c D_\varepsilon$

$V = \frac{D_\varepsilon}{W} \log \left(1 + \frac{Wy}{D_\varepsilon} \right)$

This general solution reduces to the well known linear-parabolic equation when gasflow is absent:

$$\frac{y^2}{D} + \frac{2y}{K} = \frac{2\Omega_{th}C\phi.t}{\bar{v}} \quad (14)$$

In case diffusion is absent equation 13 reduces to

$$y^2 P_c + \frac{2\bar{v}\varepsilon}{K} y = \frac{2\Omega_{th} C \varepsilon \phi . t}{1 - \varepsilon} \quad (15)$$

It may be noted that also the gasflow equation 15 is linear-parabolic. The temperature dependence of eq. 15 is weak and only present in the linear part, meaning when y is very small. With thicker oxide layers the gasflow through the pores behaves parabolic because of the collisions of the atoms with the wall of the pore. The diffusion equation 14 has the temperature dependence both in the linear and in the parabolic part. It demonstrates that at low temperatures the gasflow through the pores is the dominating process, while at high temperature the diffusion is rate controlling.

Results

To establish the constants used in eq. 13 data is used from atomic oxygen exposure tests in low earth orbit, from atomic oxygen experiments on ground and from oxygen plasma exposure tests. The total silver loss during the STS-8 flight was measured as 3 μm to 4.5 μm . (approx. 2½ μm to 3½ μm at the front and ½ μm to 1 μm at the rear side of the silver sample due to reflected atomic oxygen). As illustrated in figure 3 the oxide can flake off and thus exposing underlying silver, which is oxidised again. The oxide flakes have a thickness of ½ μm to 2 μm . This increases the silver loss.

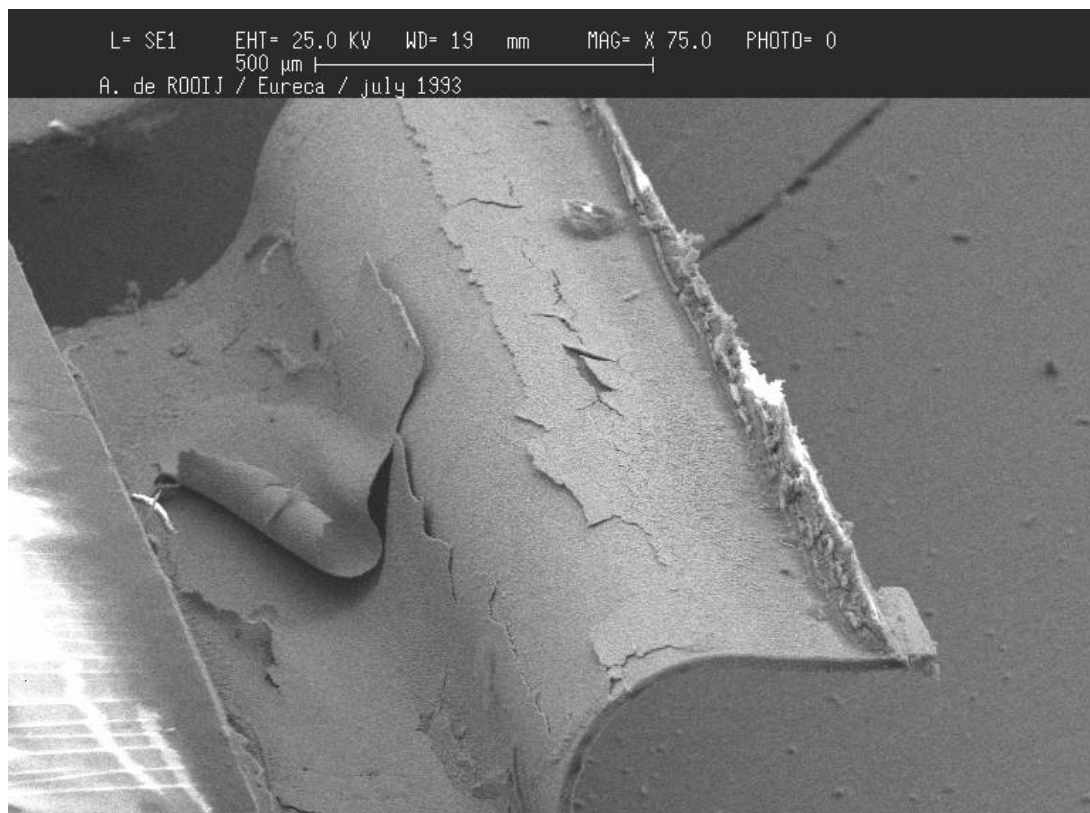


Figure 3: Silver interconnector (34 μm) retrieved from Eureka. It shows oxidised silver which is flaked off and exposing the underlying fresh material which is oxidised again

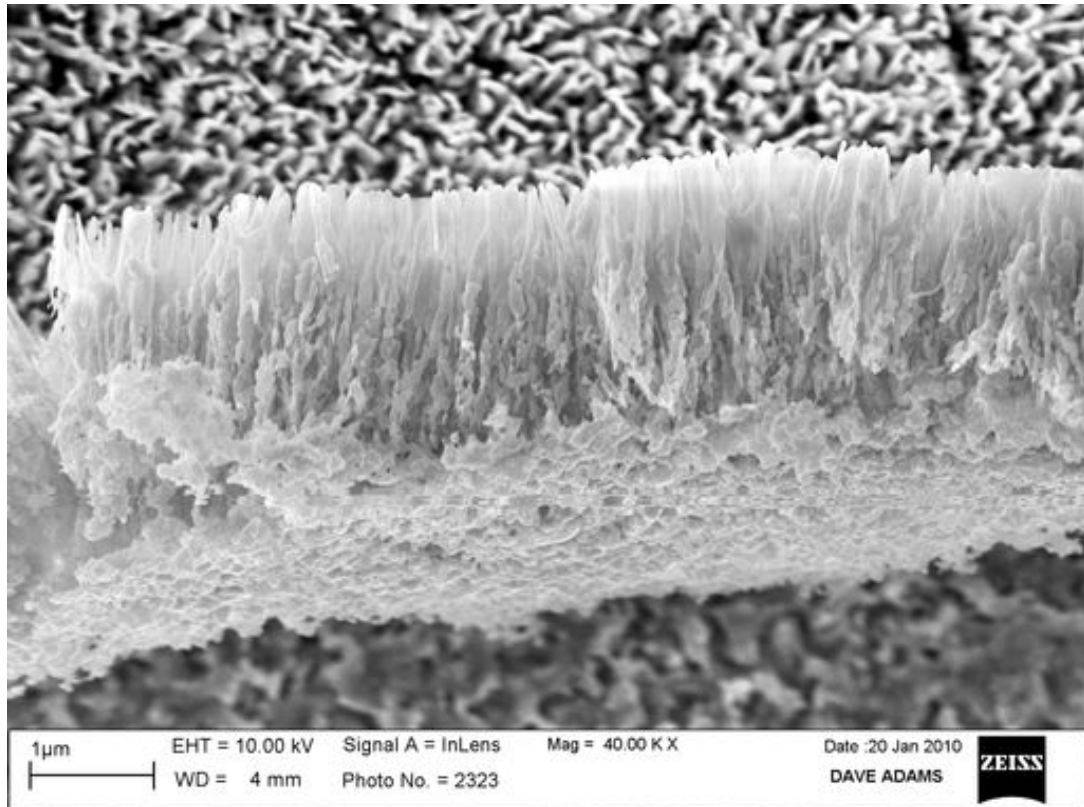


Figure 4: Cross section of silver-oxide flake showing the pore structure

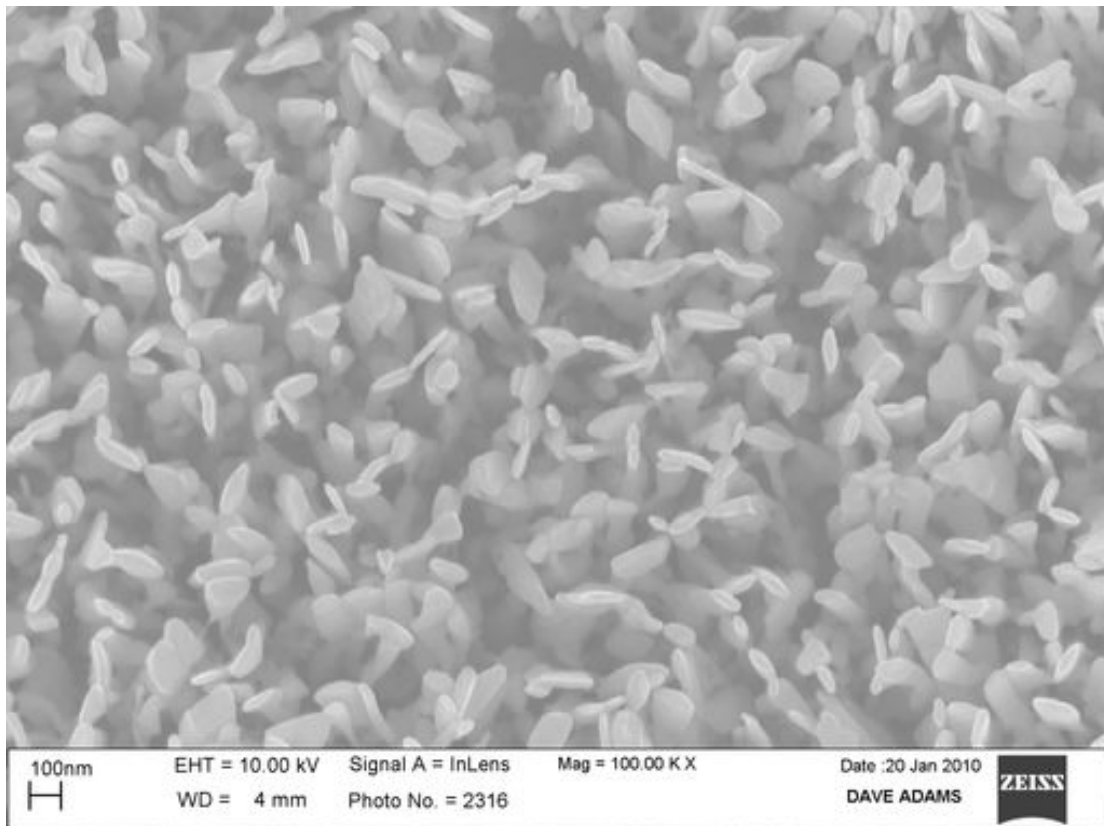


Figure 5: Oxidised silver surface from which the average pore surface area and perimeter is calculated using image analysis software

To account for that it is assumed that the silver loss occurred in several stages each producing flakes of the same thickness making up the $2\frac{1}{2} \mu\text{m}$ to $3\frac{1}{2} \mu\text{m}$ silver loss. The conditions during the exposure of the silver samples were measured as:
 Atomic oxygen impact energy = 5 eV with a substrate temperature = 77 °C
 Fluence = $3.5 \cdot 10^{20}$ atoms/cm² during the 40 hrs of exposure.

The oxide/metal ratio Ω_r was found to be 2 from oxygen plasma exposure tests and according eq. 11 this gives a porosity $\varepsilon = 0.2$. The oxygen plasma exposure tests were performed for different exposure times. The temperature of the samples was not controlled but temperature indicators on the rear side of the sample indicated a maximum temperature of 85 °C. The results are shown in figure 6. The values used in the pores characterisation is measured using oxygen plasma experiments and atomic oxygen experiments using the ESTEC atomic oxygen facility. From the cross section of a silver-oxide flake the pores are visible and the real length can be measured and related to the thickness of the oxide itself, as illustrated in figure 4. The tortuosity τ is then calculated as $\tau = 1.2$. The pores in the silver-oxide are rather straight. The average pore cross section and perimeter are measured on scanning microscope photos using the Clemex image analysis software as shown in figure 5. The hydraulic radius $2A/H$ is measured as 38 nm. Exposure experiments conducted in the ESTEC atomic oxygen facility are performed at room temperature and resulted in an oxide thickness of 1.5 μm at a fluence of $3.1 \cdot 10^{20}$ atoms/cm². The thicknesses of the oxides are measured using a LEO confocal microscope. The fluences are calculated from Kapton HN samples exposed to the oxygen plasma or atomic oxygen beam at the same time as the silver samples. The degradation of the Kapton HN is used as calibration, while the degradation of Kapton HN under atomic oxygen attack in low

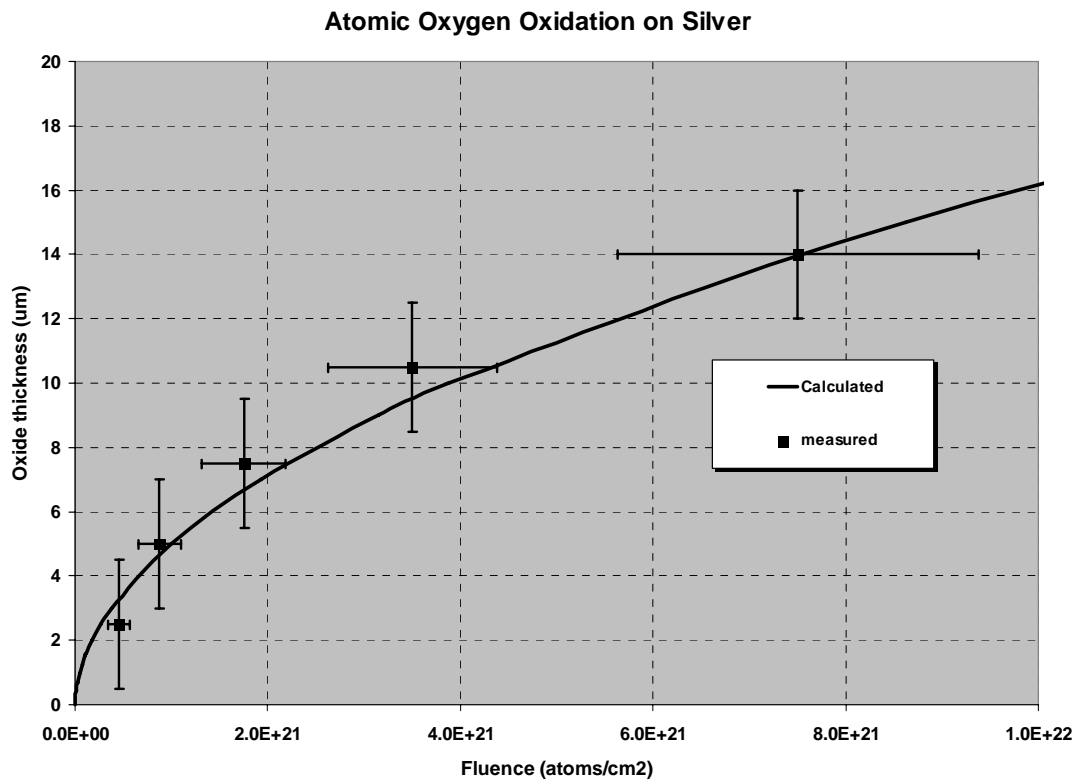


Figure 6: Experimental results from oxygen plasma tests on silver. The solid line represents eq. 13 using constants to fit the data to the experimental results

earth orbit is well characterised.

The constants in eq. 13 are determined using the room temperature measurement in the atomic oxygen beam facility and using the results from the oxygen plasma exposure at 85 °C as given in figure 6. The solid line represents eq. 13, using: $D_o = 5.28 \cdot 10^3 \text{ cm}^2/\text{s}$, $K_o = 5.28 \cdot 10^8 \text{ cm}^2/\text{s}$, $Q = 3.3 \cdot 10^4 \text{ J/mol}$, $H/A = 5.263 \cdot 10^{-3} \text{ nm}^{-1}$, $\tau = 1.2$ and $\varepsilon = 0.2$.

Conclusion

The transport of oxygen through the oxide layer is modelled using two transport mechanisms, namely gas flow through micro-pores and Fickian diffusion. The interfacial reaction between oxygen and silver is taken as linear, resulting in a linear-parabolic oxidation with flux and time. Because the two mechanisms are separated one can investigate the contributions of both transport mechanisms to the oxidation of silver. The model results in a low-temperature oxidation by gas flow while at higher temperature the diffusion mechanism controls the kinetics of the oxidation. Both the Fickian diffusion and the gas flow through the micro pores are exhibit parabolic growth. For the Fickian transport the diffusion is inversely proportional to the thickness of the oxide layer. For the gas flow transport the flow resistance, for a gas with a mean free path much larger than the pore dimension, is inversely proportional to the length of the micro-pore.

Flaking and spalling of the oxide layer has a large impact on the oxidation of the surface. The flaking and spalling of the oxide layer due to internal stresses in the oxide layer results in a continuously restarting of the oxidation process. In the model it is assumed that flaking is absent, but can easily be introduced by assuming a constant flake thickness. When the oxide layer reaches this thickness it will flake off, leaving bare metal exposed to the atomic oxygen environment. This oxidation process will result more or less in a linear surface attack.

References

1. Bruce A. Banks, et al., *Atomic Oxygen Effects on Spacecraft Materials*. NASA/TM—2003-212484, 2003.
2. Daniel R. Peplinski and Graham S. Arnold. *Introduction to: Simulation of Upper Atmosphere Oxygen Satellite Exposure to Atomic Oxygen in Low Earth Orbit*. in *13th Space Simulation Conference*. 1984. Orlando, Florida.
3. Hedin, A.E., *MSIS-86 Thermospheric Model*, J. Geophys. Res. , 1987. **A5(92)**: p. 4649.
4. de Rooij, A., *The Oxidation of Silver by Atomic Oxygen*. ESA Journal, 1989. **13**: p. 363-382.
5. A. R. Chambers, I. L. Harris, and G. T. Roberts, *Reactions of spacecraft materials with fast atomic oxygen*. Materials Letters, 1996. **26**: p. 121-131.